Electronic Supplementary Material (ESI) for Materials Horizons.

Supplementary Materials for

Programmable and Resilient Mechanical Metamaterials with Anisotropic and Non-linear Mechanical Response Composed Exclusively of Stiff Constituents.

Hongyi Yao[#], Xiaoyu Zhao[#], Kaiwen Shi, Wei Sun and Shengli Mi

Corresponding author: mi.shengli@sz.tsinghua.edu.cn

1 Procedural modelling of the MCC

1.1. Overview

Procedural modelling is an automated modelling method. Based on this, one can build complex 3D geometric models by assembling basic geometric elements, such as points, curves, and surfaces. This procedure gives these geometric models programmability, that is, a finite number of principal parameters drive continuous changes of the model geometry.

The design architecture of the MCC can be divided into three layers. The first is the basic layer, whose elements are the arc-serpentine curved beam pairs (ASCBP). The second is the derivative layer including "ribbon" and "frame" structures which are derived from the ASCBP. The third is the model layer consisted of the MCC, an ortho-polyhedral metastructure assembled by several frames interconnected via ribbons. Without loss of generality, the orthopolyhedron adopted in this manuscript is the orthohexahedron (cube).

The modelling of MCC is a decomposing-reconstruction process as follows:

1) Decompose a cube of dimension A (mm) into six scalable facets and shrink them to size a (mm) while maintaining their positions and orientations.
2) Transform the shape of six shrunken facets into a chosen type of frames.
3) Connect frames with eight ribbons to form an MCC.

In the above steps, step-1 implements the top-down decomposition of a cubic template, and steps-2 and -3 implement the programmatic modelling The design of the ASCBP as a basic layer element is described in detail in subsection 2. Based on this, the ribbon generation algorithms for the frames in step-2 and step-3 are briefly described in subsections 3 and 4, respectively. Finally, the coupling

algorithm for determining the number and distribution of ribbons (i.e. which two frames are connected by a ribbon) is described in subsection 5.

1.2. The geometry of ASCBP

The arc-serpentine curve (ASC) is a composite curve consisting of two circular arcs, combined by a serpentine, with equal curvatures. The curve is centered on the serpentine and has an arc of equal curvature but opposite direction at the beginning and end of the curve. Compared to the traditional serpentine, the serpentine curve retains its central symmetry (i.e., handedness), but discards the straight section in the central region and replaces it with a circular arc. Consequently, an ASC beam (ASCB) is a curved beam derived from sweeping an ASC with a rectangular cross section whose ratio of width to thickness is β.

A single arc serpentine curve can be subdivided into four circular arc segments of equal curvature. Based on this fact, we built the mathematical model of the curve in complex domain. Firstly, the four arc segments A_j^0 $(j = 1,2, ...4)$ with the origin center can be expressed as:

$$A_j^0 = \rho_j e^{i(\varphi_j + sign(2.5-j)t_j)I_h} \tag{1-1}$$

where ρ_j, φ_j and t_j are the radius of curvature, phase angle and position parameters related to the j th arc segment. Besides φ_j satisfies the iterative relation:

$$\varphi_{j+1} = \varphi_j + \gamma_j\theta_j - 0.5\pi\left(1 - \gamma_j\gamma_{j+1}\right) \tag{1-2}$$

In particular, we defined $\varphi_1 = [1,1,-1,-1]$ as a vector of the signs of the curvature of each arc segment. θ_j is the central angle of the jth circular arc, and $t_j \in [0, \theta_j]$. I_h is the chiral indicative value. The ASC whose $I_h = 1$ is defined as a left-handed curve. Conversely, the ASC of $I_h = -1$ is the right-handed counterpart.

Secondly, the four arc segments are translated in a serial manner with their heads and tails connected. So, the circular arc segment after the translation is $A_j(t_j)$:

$$A_{j+1}(t_{j+1}) = A_{j+1}^0(t_j) - A_{j+1}^0(0) + A_j^0(\theta_j) \tag{1-3}$$

Finally, the expressions of the connected segments are summed as:

$$G(t) = \sum_{j=1}^{4} \delta_{jl} A_j \left(t - \sum_{k=1}^{l} \theta_k \right) \tag{1-4}$$

where $t \in \left[0, \sum_{j=1}^{4} \theta_j\right], l = 5 - \sum_{j=1}^{4} \left\lfloor \min\left\{\sum_{k=1}^{j} \theta_k, k\right\}/t \right\rfloor$. For an arc serpentine curve to be internally tangent to a square, the radius ρ_j of each circular segment and the angle θ_j of the center of the circle need to satisfy the following relationship:

$$\begin{cases} \theta_2 = \theta_3 \\ \rho_1 = \rho_4 \end{cases} \tag{1-5}$$

At this point, we established the mathematical model of standard ASC.

Next, the extended ASC will be described. We added adds a circular arc segment to the standard ASC at its beginning/end and received extended ASC. This segment can be in or out of the complex plane, forming a coplanar expanded arc serpentine curve (used in the frame case) and a non-coplanar expanded arc curve (used in the ribbon case), respectively, with the standard ASC. Therefore, the mathematical description of the expanded ASC is the basis for subsequent work. The specific process is as follows:

1) Extend the description of the standard ASC in the complex domain to three-dimensional space. Establish a three-dimensional orthogonal coordinate system $\mathbf{C}^3 = \{(x_1, ix_2, x_3): x_j \in \mathbf{R}\ for\ j = 1,2,3\}$ and take $(\boldsymbol{e}_1, \boldsymbol{e}_2, \boldsymbol{e}_3)$ as a set of bases for $\mathbf{C}^3$, i.e. $\mathbf{C}^3 = span(\boldsymbol{e}_1, \boldsymbol{e}_2, \boldsymbol{e}_3)$,where $\boldsymbol{e}_1 = (1,0,0), \boldsymbol{e}_2 = (0, i, 0), \boldsymbol{e}_3 = (0,0,1)$.

2) The standard ASC is constructed in the plane of the $\boldsymbol{e}_1$and$\boldsymbol{e}_2$ expansions according to the above process, i.e. $G(t) \in span(\boldsymbol{e}_1, \boldsymbol{e}_2)$.

3) For a coplanar expanding ASC, a segment of coplanar arc of equal curvature extends smoothly from the end/head of the standard left/right-handed circular arc curve. Denote this type of circular arc segment as coplanar arc segment A_c . The corresponding circular central angles and radius of curvature are $\rho_c$and θ_c respectively:

$$A_c(t_c) = \rho_c e^{i(\varphi_c - t_c)I_{\hbar}} + \frac{\left(I_{\hbar} + 1\right)}{2} G\left(\sum_{j=1}^{4} \theta_j\right) \# \tag{1-6}$$

where $t_c \in [0, \theta_c]$, and:

$$\varphi_c = \begin{cases} \varphi_4 + \theta_4, \ for\ I_{\hbar} = 1 \\ 0, \ for\ I_{\hbar} = -1 \end{cases} \# \tag{1-7}$$

Thus, in $\mathbf{C}^3$, the parametric mathematical model for the coplanar expanding arc serpentine curve is $\boldsymbol{G}_c(t) = \left(\mathbf{Re}\left(G_c(t)\right), i\mathbf{Im}\left(G_c(t)\right), 0\right)$

where:

$$G_c(t) = \begin{cases} G(t), \ for\ t \in \left[0, \sum_{j=1}^{4} \theta_j\right] \\ A_c\left(t - \sum_{j=1}^{4} \theta_j\right), \ for\ t \in \left(\sum_{j=1}^{4} \theta_j, \sum_{j=1}^{4} \theta_j + \theta_c\right] \end{cases} \tag{1-8}$$

4) For a non-coplanar extended circular curve, an isocurvature non-coplanar arc A_b extends smoothly from the end/head of the standard left/right-handed circular curve. The angle between the plane in which A_b lies and the plane in which A_c lies is θ_r . The corresponding angle of centre and radius of curvature of this arc are ρ_b and θ_b respectively.

To facilitate the description, the plane in which the non-coplanar circular arc segment is located is first coincident with the plane in which the circular curve is

located, at which point the mathematical description of the non-coplanar circular arc segment A_b is the same as that of the coplanar arc segment A_c, i.e.:

$$A_b(t_b) = \rho_b e^{i(\varphi_b - t_b)I_{\hbar}} + \frac{\left(I_{\hbar} + 1\right)}{2} G\left(\sum_{j=1}^{4} \theta_j\right) \# \tag{1-9}$$

where $t_c \in [0, \theta_c]$, and:

$$\varphi_b = \begin{cases} \varphi_4 + \theta_4, \ for\, I_{\hbar} = 1 \\ 0, \ for\, I_{\hbar} = -1 \end{cases} \# \tag{1-10}$$

Next is the rotation operation. Let the unit velocity vector at the end/head endpoint of the left/right standard ASC be $\boldsymbol{e}_v$ and the unit quaternion $\boldsymbol{q} = (\cos(\theta_r/2), \sin(\theta_r/2)\, \boldsymbol{e}_v)$. The rotated non-coplanar arc segment $\boldsymbol{A}_b^r(t)$ can then be derived as:

$$\boldsymbol{A}_b^r(t) = R[\boldsymbol{q}\left(1, \boldsymbol{Re}\left(A_b(t)\right), \boldsymbol{Im}\left(A_b(t_b)\right), 0\right)\boldsymbol{q}^*] \tag{1-11}$$

where $R[\cdot]$ is the part of the vector that takes the corresponding quaternion.

Thus, in $\mathbf{C}^3$, the parametric mathematical model for the non-coplanar expanded arc serpentine curve is:

$$\boldsymbol{G}_b(t) = \begin{cases} \left(\boldsymbol{Re}\left(G(t)\right), i\boldsymbol{Im}\left(G(t)\right), 0\right), \ for\, t \in \left[0, \sum_{j=1}^{4} \theta_j\right] \\ \boldsymbol{A}_b^r, \ for\, t \in \left(\sum_{j=1}^{4} \theta_j, \sum_{j=1}^{4} \theta_j + \theta_c\right] \end{cases} \# \tag{1-12}$$

At this point, the mathematical models for both forms of the expanded arc serpentine curve have been built.

Further, we will construct pairs of ASCB (ASCBP) from pairs of ASCs. The first endpoint of any right-handed arc serpentine curve is translated to coincide with the endpoint of a left-handed arc serpentine curve with the same parameters (radius of curvature and centre angle), and the connection is kept smooth (i.e. the velocity vectors of the two ASCs at the point of contact are kept the same by

pre-rotation before translation). The composite curve formed by this rotation-translation operation is defined as the arc serpentine curve pair. With this as the neutral axis and the rectangle as the cross-section, the arc serpentine curve pair is swept into shape. In addition, to prevent off-surface instability of the ASCs, β ,the ratio of the width W to the thickness T is taken to be 4 for ribbon, 2 for frame and the thickness $T = 1.5\ mm$. These three pairs form the base layer of the MCC cascade architecture. On their basis, we construct the derived layer, as described in subsections 3 and 4.

1.3. Generation of frame structure (ASCBP type)

The frame structure (ASCBP type) is a square composed of several ASCBPs. Obviously, the conversion of a square made of straight lines into a frame made of ASCBP is the core of the entire structure generation process. To refine this, it is necessary to determine the type, size, number, and position of the corresponding ASCBP according to the length of the sides of the square. There are two types of ASCBP used in this part of the method, the standard pair and the coplanar expansion pair.

For the sake of brevity, the relevant parameters are defined here. The minimum ASCB size allowed by the actual process is ρ_{min} ; the number of ASCBP's contained in a quarter of the frame is $n_{0.25}$; as the standard ASC has a square cut into it, the side length ρ of the square is the corresponding ASCBP size; the half length of the square template is $L = a/2$.

The specific generation process is as follows:

1) Decompose the four sides of the square template into four identical fold segments by taking the midpoints of the four sides of the square and carrying out the following steps using the first quadrant fold segment as an example.

2) The number of ASCBP required for a rough calculation of the folded segment $\overline{n}_{0.25}$:

$$\overline{n}_{0.25} = 2\left\lfloor \frac{\beta_f - 1}{2} \right\rfloor - 1\# \tag{1-13}$$

where β_f is the length scaling factor:

$$\beta_f = \frac{L}{\rho_{min}} - 0.5\# \tag{1-14}$$

3) Rough calculation of ASCBP size $\overline{\rho}$:

$$\overline{\rho} = \frac{L}{\overline{n}_{0.25} + 0.5}\# \tag{1-15}$$

4) Verify the validity of $\hat{\rho}$ and determine the final number of ASCBP's $n_{0.25}$:

$$n_{0.25} = \begin{cases} \overline{n}_{0.25},\ for\ \hat{\rho} \geq \rho_{min} \\ \overline{n}_{0.25} - 2,\ for\ \hat{\rho} < \rho_{min} \end{cases}\ \# \tag{1-16}$$

5) Calculate the ASCBP final size ρ_f:

$$\rho_f = \frac{L}{n_{0.25} + 0.5}\# \tag{1-17}$$

In the framework structure, we set $\rho_1 = \rho_c = \rho_f$ and $\theta_1 = \theta_c = \pi/4$.

6) If $n_{0.25} = 1$, then only one coplanar expansion pair needs to be generated; if $n_{0.25} > 1$, then only one coplanar expansion pair needs to be generated at the same time, along with $n_{0.25} - 1$ standard pairs. In this case, the standard pairs are connected uniformly symmetrically and smoothly to the first and last endpoints of the coplanar expansion pair.

7) Repeat steps 2-6 for the remaining quadrant of the folded segments. When complete join the four sets of arc-snake curve pairs in sequence to form a smooth closed curve and use this as the neutral axis to form the body of the frame structure by sweeping as described in subsection 2.

8) Add an octagonal connector with an internal diameter of 2.2mm to the center of each serpentine beam.

With the above algorithm, we can convert any square template into a frame and ensure that the sides of the square pass through the geometric centers of all the curves of the frame. The converted body of the frame remains square, and the side length becomes $a + \rho$ and the thickness βT.

1.4. Generation of ribbon structure (ASCBP type)

A ribbon structure is a spatial structure, whose shape is similar to a corner piece, consisting of ASCBPs. Similarly, to the frame structure, the conversion of vertical folded segments made up of straight lines into ribbon structures made up of ASCBP is the core mission of this generation process. Specifically, the mission to determine the types, sizes, numbers, positions and orientations of the corresponding ASCBPs based on the geometry of the given vertical folds. There are two types of ASCBP involved in this part of the method, the standard pair (type-I) and the non-coplanar expanded pair (type-II). Unlike frame structures, which are converted at square corners using co-planar expansion pairs, ribbon structures are converted at vertical bends with non-coplanar expanded pairs. This treatment ensures the alignment of the normal vectors between the ribbon and the frame at the joint interface.

Again, we define relevant parameters first. Denote the minimum ASCB size allowed by the actual process as ρ_{min}; the number of ASCBP contained in a ribbon as n_1; the size of the resulting ASCBP as ρ; and the radius of the non-coplanar arc $\rho_b = \omega_c \rho_f$,where ω_c is the radius scale factor. This is a tunable parameter with a default value of 1. The coordinates of the start, end and intersection points of the vertical dash are noted as $\boldsymbol{P}_a$, $\boldsymbol{P}_b$ and $\boldsymbol{P}_c$ and the velocity vectors at the start and end points are $\boldsymbol{V}_a$ and $\boldsymbol{V}_b$ respectively.

The specific process is as follows:

1) Calculate $\boldsymbol{P}_c = F(\boldsymbol{P}_a, \boldsymbol{P}_b, \boldsymbol{V}_a, \boldsymbol{V}_b)$ according to the classical intersection searching algorithm.

2) Therefore, the area of radius ρ_b around the intersection point (fold corner) needs to be set aside separately for the generation of out-of-plane expanding circular beams in the rough calculation of the number of ASCBP required. With this, the number of ASCBP required for the rough calculation of the folding segments, $\overline{n}_1$, is

$$\overline{n}_1 = 2\left\lceil \frac{\beta_r}{2.5} \right\rceil - 1\# \tag{1-18}$$

where β_r is:

$$\beta_r = \frac{\|\boldsymbol{P}_c - \boldsymbol{P}_a\| - \rho_b}{\rho_{min}} \tag{1-19}$$

Note that the two sides of the vertical fold segment to be converted in the scenario in this paper are of equal length, thus $\|\boldsymbol{P}_c - \boldsymbol{P}_a\| = \|\boldsymbol{P}_c - \boldsymbol{P}_b\|$. Therefore, for more generalised conditions, the two side lengths need to be calculated separately for each $\overline{n}_1$.

3) Rough calculation of ASCBP size $\overline{\rho}$:

$$\overline{\rho} = \frac{\|\boldsymbol{P}_c - \boldsymbol{P}_a\|}{\overline{n}_1 - 0.5} \tag{1-20}$$

4) Verify the validity of $\hat{\rho}$ and determine the final number of ASCBP, n_1:

$$n_1 = \begin{cases} \overline{n}_1, \ for\ \hat{\rho} \geq \rho_{min} \\ \overline{n}_1 - 2, \ for\ \hat{\rho} < \rho_{min} \end{cases} \tag{1-21}$$

5) Calculate the final size of the ASCBP ρ_r:

$$\rho_r = \frac{\|\boldsymbol{P}_c - \boldsymbol{P}_a\|}{n_1 - 0.5} \tag{1-22}$$

In the ribbon, we set $\rho_1 = \rho_r$ and $\theta_1 = \theta_b = \pi/4$.

6) If $n_1 = 1$, only one non-coplanar expanded pair is generated; if $n_1 > 1$, one non-coplanar expanded pair and $n_1 - 1$ standard pairs are generated. In this

case, the standard pairs are connected uniformly symmetrically and smoothly to the first and last endpoints of the non-coplanar expanded pair. This is then used as the neutral axis to form the body of the ribbon by sweeping as described in subsection 2.

7) Unlike the frame, an octagonal connector with an internal diameter of 2.2mm is added at the centre of the first and last ASCBs for modular case.

With the above algorithm, we can convert a given vertical fold segment into a ribbon and ensure that the vertical fold passes through the geometric center of the ribbon's first and last arc snake curves. The converted ribbon body is "L" shaped and has an overall length of $2\|\boldsymbol{P}_c - \boldsymbol{P}_a\| + \rho + \rho_b\pi/4$ and a thickness of βT.

At this point, we have described the rules for the generation of the basic elements (frames and ribbons) of the second derivative layer of the cascade architecture. In the third model layer, the two elements are stacked and assembled in a given number and distribution to form the final MCC, obviously with the number and position of the frames corresponding to the six square templates. And the way in which these six frames are connected to each other by ribbons determines the number, position and attitude of the ribbons in a single MCC. In this document, this information is given in the connection table. The contents of the connection table and the algorithm used to generate it therefore directly determine the topology and corresponding mechanical properties of the entire MCC.

1.5. Algorithm of generating connection tables

For documentation and description purposes, it is necessary to define the face number I_f for all frames in a single MCC, followed by the point number I_p for the interfaces in a single frame, each of which is an integer and must be unique. The face number can take the value range $I_f \in [0,5]$, which is not specific and can be generated randomly. The point number range $I_p \in [0,8n_{0.25} - 1]$ is

defined in the order in which the arc-snake pairs are generated in the individual frames described in subsection 3, i.e. starting with the arc serpentine curve closest to the Y-axis in the first quadrant and proceeding clockwise from 0. The interface reference syntax is defined as interface $I_f - I_p$. For example, interface 2-0 indicates an interface with point number 0 in a frame with face number 2. It should be noted that only the interfaces of the co-planar expanded pairs in this chapter are used for assembly with ribbons in the frame, and all interfaces in subsequent content refer to such interfaces.

Before generating the connection table, it is necessary to calculate the tangent connection matrix $\boldsymbol{T}$ First, the nearest neighbour interfaces for each interface are calculated and form a $6 \times 8n_{0.25} \times 2$ three-dimensional matrix $\boldsymbol{H}$. H_{ij1} denotes the point number of the nearest neighbour interface for the $i - j$ interface (the interface with point number j in the frame with face number i); similarly, H_{ij2} denotes the point number of the nearest neighbour interface for the i-j interface (the interface with point number j in the frame with face number i) of the nearest neighbouring interface. Next, the three-dimensional matrix $\boldsymbol{T}$ is calculated by deriving from $\boldsymbol{H}$.

$$\begin{cases} T_{ij1} = H_{ij1} + (-1)^{\lceil 0.5H_{ij1} \rceil - 1} \\ T_{ij2} = H_{ik2} \end{cases} \tag{1-23}$$

where $k = j + (-1)^{\lceil 0.5H_{ij1} \rceil - 1}$. On the basis of $\boldsymbol{T}$, the connection table is generated. In the initial state, all interfaces are available and the corresponding state indicator $I_j = 0$ When any interface is recorded in the connection table, its $I_j = 1$, indicating that the interface is used. At the same time, the state indicator of the interface's neighbouring interfaces in the same co-planar expanded pair, and the corresponding interface in H, becomes $I_j = -1$, indicating that the interface is disabled and does not enter the connection table (i.e.

two pairs are disabled while one pair is credited). The specific algorithm is as follows.

1) Starting from the frame with face number 0, the interfaces with an even number of point numbers are connected to their corresponding interfaces by $\boldsymbol{T}$ and recorded in the connection table. Each correspondence occupies one row of the connection table, and the elements of each row are the starting interface and the target interface, in that order.

2) For frames with a non-zero face number, a judgement needs to be made based on the number of used holes. If the number of used interfaces is 1 and the corresponding centrosymmetric interface $I_j = 0$ located on that frame, the centrosymmetric interface and its corresponding interface in T will be recorded in the connection table; if the number of used interfaces is greater than 1, the interfaces with the smallest point number among all available interfaces will be recorded in the connection table in turn. It is important to note that each time a connection is entered into the connection table, the smallest point numbered interface is re-evaluated. When the number of available interfaces in the frame is zero, jump to the next frame and repeat step 2.

3) When all frames have completed their pairing work, the algorithm ends and the join table is generated.

For the cube MCC, the corresponding $\boldsymbol{H}$, $\boldsymbol{T}$ are:

$$H_{..1} = \begin{bmatrix} 3 & 6 & 5 & 0 & 7 & 2 & 1 & 4 \\ 3 & 0 & 7 & 0 & 7 & 0 & 7 & 4 \\ 3 & 2 & 1 & 0 & 7 & 6 & 5 & 4 \\ 3 & 4 & 3 & 0 & 7 & 4 & 3 & 4 \\ 5 & 6 & 5 & 6 & 5 & 6 & 5 & 6 \\ 1 & 2 & 7 & 2 & 1 & 2 & 1 & 2 \end{bmatrix} \tag{1-24}$$

$$H_{..2} = \begin{bmatrix} 1 & 5 & 5 & 3 & 3 & 4 & 4 & 1 \\ 2 & 5 & 5 & 0 & 0 & 4 & 4 & 2 \\ 3 & 5 & 5 & 1 & 1 & 4 & 4 & 3 \\ 0 & 5 & 5 & 2 & 2 & 4 & 4 & 0 \\ 1 & 0 & 0 & 3 & 3 & 2 & 2 & 1 \\ 1 & 2 & 2 & 3 & 3 & 0 & 0 & 1 \end{bmatrix} \tag{1-25}$$

$$T_{..1} = \begin{bmatrix} 7 & 2 & 1 & 4 & 3 & 6 & 5 & 0 \\ 1 & 2 & 1 & 6 & 1 & 6 & 5 & 6 \\ 3 & 2 & 1 & 0 & 7 & 6 & 5 & 4 \\ 5 & 2 & 1 & 2 & 5 & 6 & 5 & 2 \\ 7 & 4 & 7 & 4 & 7 & 4 & 7 & 4 \\ 3 & 0 & 3 & 0 & 3 & 0 & 3 & 0 \end{bmatrix} \tag{1-26}$$

$$T_{..2} = \begin{bmatrix} 5 & 1 & 3 & 5 & 4 & 3 & 1 & 4 \\ 5 & 2 & 0 & 5 & 4 & 0 & 2 & 4 \\ 5 & 3 & 1 & 5 & 4 & 1 & 3 & 4 \\ 5 & 0 & 2 & 5 & 4 & 2 & 0 & 4 \\ 0 & 1 & 3 & 0 & 2 & 3 & 1 & 2 \\ 2 & 1 & 3 & 2 & 0 & 3 & 1 & 0 \end{bmatrix} \tag{1-27}$$

The corresponding ribbons are generated in sequence according to the generation table shown in Table S1 and are assembled with the frames in a stacked fashion through the interfaces of the corresponding serial numbers.

TableS1 The connection table of MCC

Starting interface	Target interface
0-0	5-7
0-2	3-1
0-4	4-3
0-6	1-5
1-1	2-2
2-6	3-5
2-0	5-3
4-7	2-4

2 Methods and Materials

2.1. Simulation of the MCC compression process

In order to improve the efficiency of the simulation, two simplifications were made to the geometry of the MCC: firstly, the complex features on the frame and ribbon were replaced with first class sized cylinders; secondly, the assembly gap between the generic interface and the frame to which it is attached was removed and transformed into a one-piece model. The simplified model was then imported in stl format from Houdini into COMSOL for finite element analysis. The geometric model was meshed with tetrahedral cells. The material model is a linear elastic model with a Young's modulus of 2108.2 MPa and a Poisson's ratio of 0.3. The body of the MCC is defined as the structural mechanics domain and the six connecting tubes as the multi-body dynamics domain, which are coupled to each other by hinge pairs to achieve multi-physics fields. A symmetric displacement boundary condition (20 mm) is applied to the corresponding connecting tube sections in the Z-axis (or X-axis) direction. A multi-step solution method is used to calculate the steady-state solution for this non-linear deformation. Also, due to the large rotation angle in the model deformation, the effect of geometric non-linearity is considered, and the strain metric is Green's strain, accordingly the stress metric is the type II Piola-Kircoff stress.

2.2. Simulation experiments with ribbons

The six MCC ribbons in the text were used as the object of study and the mesh was divided to create the simulation model. For each structure, as shown in Fig.S9, all degrees of freedom are fixed for the lower right connection hole, and this is used to apply displacement and rotation to the upper left connection hole in turn. The material model is a linear elastic model with a Young's modulus of

2108.2 MPa and a Poisson's ratio of 0.3. A multi-step solution is used to calculate the steady-state solution for this non-linear deformation. Also, due to the large rotation angle in the deformation of the model, the effect of geometric non-linearity is considered and the strain metric is Green's strain, accordingly the stress metric is the type II Piola-Kircoff stress.

2.3. Geometrical parameters and manufacturing of general joints and connection tubes

The general joint has the shape of a cylindrical body with two stepped sections. The lower, larger cylinder is used for docking with the frame structure. The upper curved recess and the cylindrical recess are used to secure the connection. The upper, smaller cylinder is used to connect the LEGO parts (1x2 smooth pin 3673) and then to complete the connection with the connecting tube, compression fittings or other universal interfaces. The connecting tube is a homogeneous cylinder with LEGO parts (1x1 hole pins) embedded at both ends and reinforced by light-curing glue. The length of the connection tube can be set according to the needs of the scenario and the task. The lengths used in this paper are 20mm and 60mm, the former being used for all work. The universal interface and the connection tube were manufactured by light-curing 3D printing (SLA X290, JUXIN, CHINA) using a conventional rigid light-curing resin material (X22) to produce the embryos. The final part is obtained after sanding and secondary curing.

2.4. Assembled MCC fabrication and compression experiments

The ribbon and frame parts are manufactured by light-curing 3D printing (SLA X290, JUXIN, CHINA) using a conventional rigid light-curing resin material (X22). After sanding and secondary curing, the final parts are produced. The six

frames and the corresponding eight ribbons were assembled using M2-18 bolts and M2 locknuts to form the corresponding MCCs (FigureS3 and FigureS4). in particular, the holes in the frames for the connections were selected according to the holes indicated in the corresponding connection tables.

To obtain a constant and uniform compression load, it is necessary to fit the MCCs with special compression heads prior to the compression test. After mounting the general joint into the frame on the corresponding face (or all faces) of the MCC, the special indenter is mounted on the face to be compressed using LEGO parts (1x2 smooth pin 3673). Similarly, a 100mm x 100mm adapter head was installed at the indenter of the pulling machine (E3000 INSTRAN). We compressed the sample to be tested at a constant speed of 5 mm/min for 30 mm and then stopped and released. It is important to note that in order to demonstrate the deformation of the MCC in compression, unlike the tests in the text, in MovieS1 and MovieS2 we compressed the sample at a constant speed of approximately 8 mm/s for 40 mm and then stopped and released. After completing one axial compression test, the sample is removed and left to rest for 3-5 minutes before switching the indenter to another surface to be tested. And so on until all tests are completed.

The data was imported into MATLAB for processing. We removed the high load segments resulting from the touching of the upper and lower frames of the MCC from the raw data. In particular, due to the large amplitude of oscillations in the raw data, a simplified graph was obtained using sampling simplification and polynomial curve fitting, and the vertical and horizontal axes of the graph were converted to equivalent force and equivalent variation. The final values of the characteristic parameters were calculated according to the relevant definitions in the text.

2.5. Compression experiments with PRMMs

A sample-specific indenter was installed at the nine common interfaces on the face of the sample to be compressed. we compressed the sample at a constant speed of 5 mm/s to a strain of 0.75~0.79 (according to different samples) and then stopped and released it back. before switching the indenter to another surface to be tested. And so on until all tests have been completed.

2.6. Compression experiments with APRMMs

Similar to the compression experiments with the MCC, the size of the special indenter for the pulling machine was increased to 300 mm x 300 mm. In addition, a sample-specific indenter was installed at the nine common interfaces on the face of the sample to be compressed. Theoretically, the compressibility of the APRMM sample should be at least three times that of the MCC, i.e. 90 mm, however this distance is much greater than the safe compression distance of the tensile machine, so we compressed the sample at a constant speed of 5 mm/s to a strain of 0.25 and then stopped and released it. After completing an axial compression test, the sample is removed and left to rest for 3-5 minutes before switching the indenter to another surface to be tested. And so on until all tests have been completed.

2.7. Manufacturing of CRUs

The two digital bus servos (LX-16A, Hiwonder, CHINA) of the CRU core drive are mounted to the core support by means of M2-8 bolts. The output gear connected to the digital bus servo has a 25T slot in the bore to form an interference fit (radial tightening) with the servo output shaft, which, together with the axial tightening of the M3-10 bolts, effectively prevents displacement and rotation between the gear and the servo. The other gear is connected to the core support by LEGO parts (1x1 hole pin and 1x2 smooth pin 3673) so that there is

only rotational freedom between the two. At the same time, the four columns on the gear are connected to a universal interface on the CRU's MCC housing, which enables the transfer of rotational power to the MCC housing.

2.8. CRUP's crawling experiment

We installed two inertial measurement units (IMU948, CHINA) on top of the two CRUs of the CRUP. The units transmit the attitude angle and angular acceleration of the connected 'frame' structure to the computer in real time via Bluetooth. For straight-line crawling, the two CRUs rotate 30° in 0.5s and recover in 0.5s. For turning crawls, the left and right CRUs rotate 20° and 30° respectively within 0.5s and recover within 0.5s. Total running time is 45s.

3 Supplementary figures

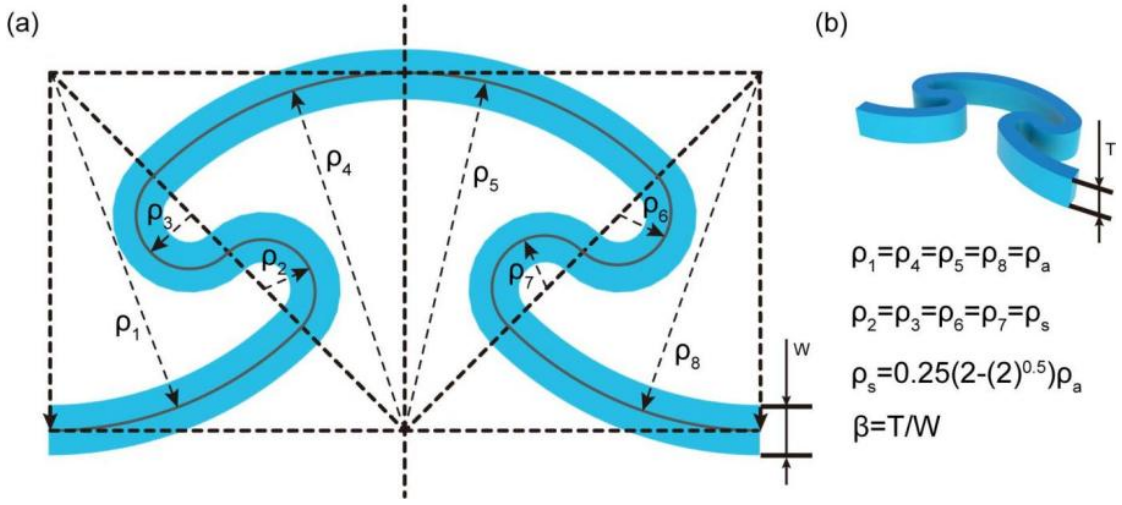

Fig. S1. Geometric definition of ASCBp. (a) Definition of the key geometric parameters. (b) The definition of ASCBp thickness and the constraint relationship between geometric parameters.

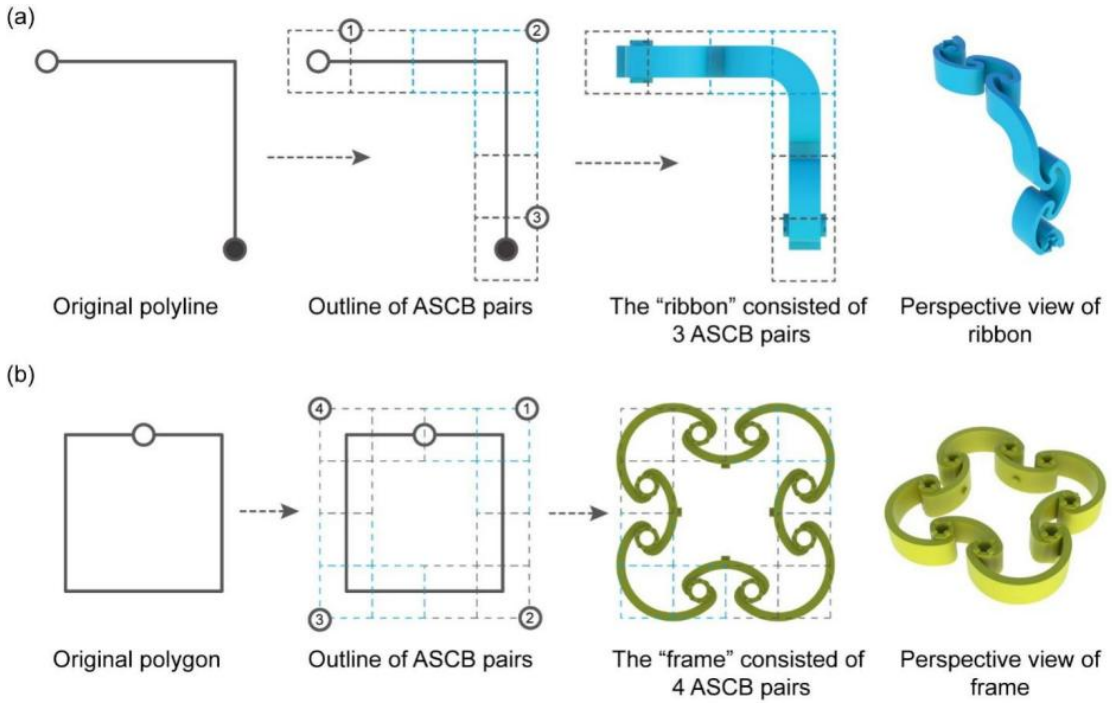

Fig. S2. Schematic diagram of the transformation process of ribbon and frame. (a) Schematic diagram of the transformation process from polyline to ribbon. (b) Schematic diagram of the transformation process from square to frame.

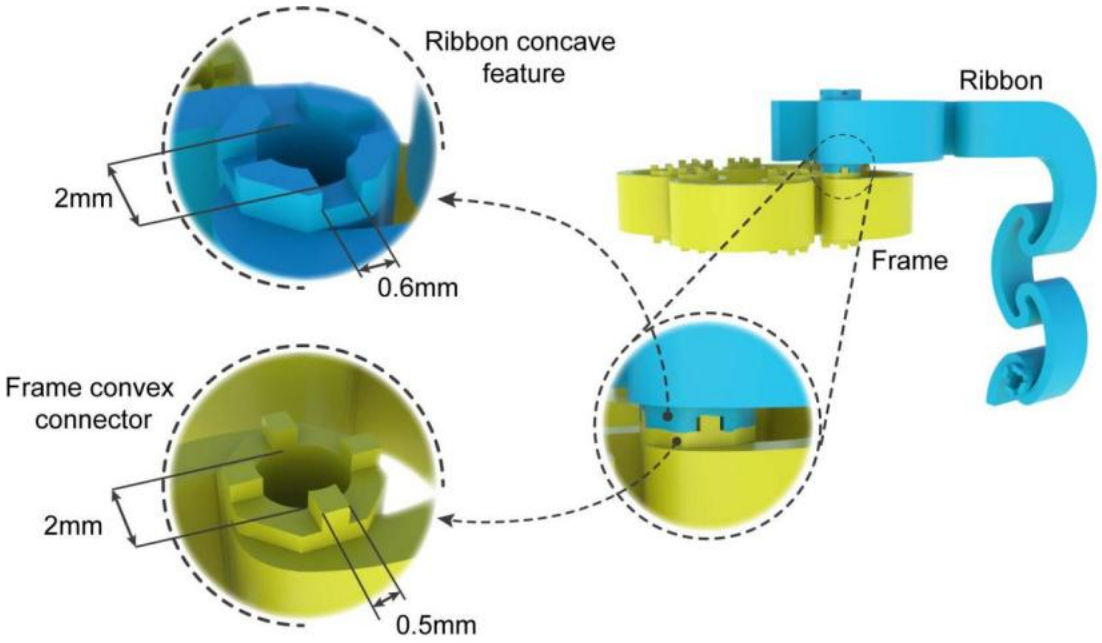

Fig. S3. Detail diagram of the geometric features used for connection on the ribbon and frame.

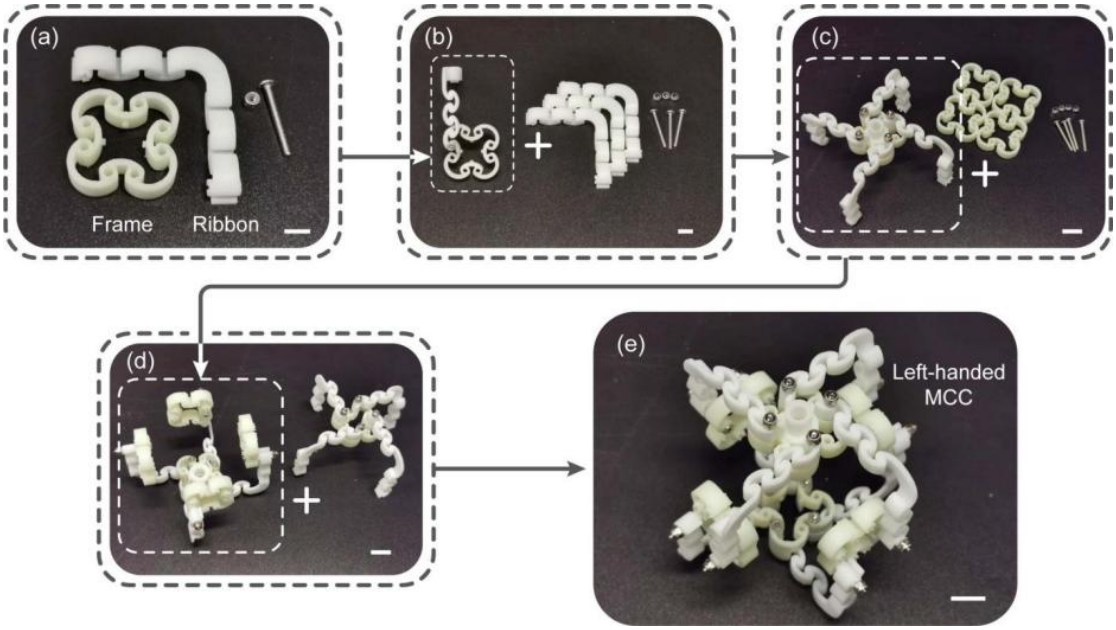

Fig. S4. Diagram of the assembly process of MCC. (a) Details of the frame and ribbon, and the bolts and locknuts required to connect the two. (b) The parts assembled in the above step with the three ribbons and the related standard parts. (c) The quadruple connected frame from the above step with the four frames and the associated standard parts. (d) The parts from the above step with another four-link frame. (e) The final assembly of the left-handed MCC with a scale bar length of 12 mm.

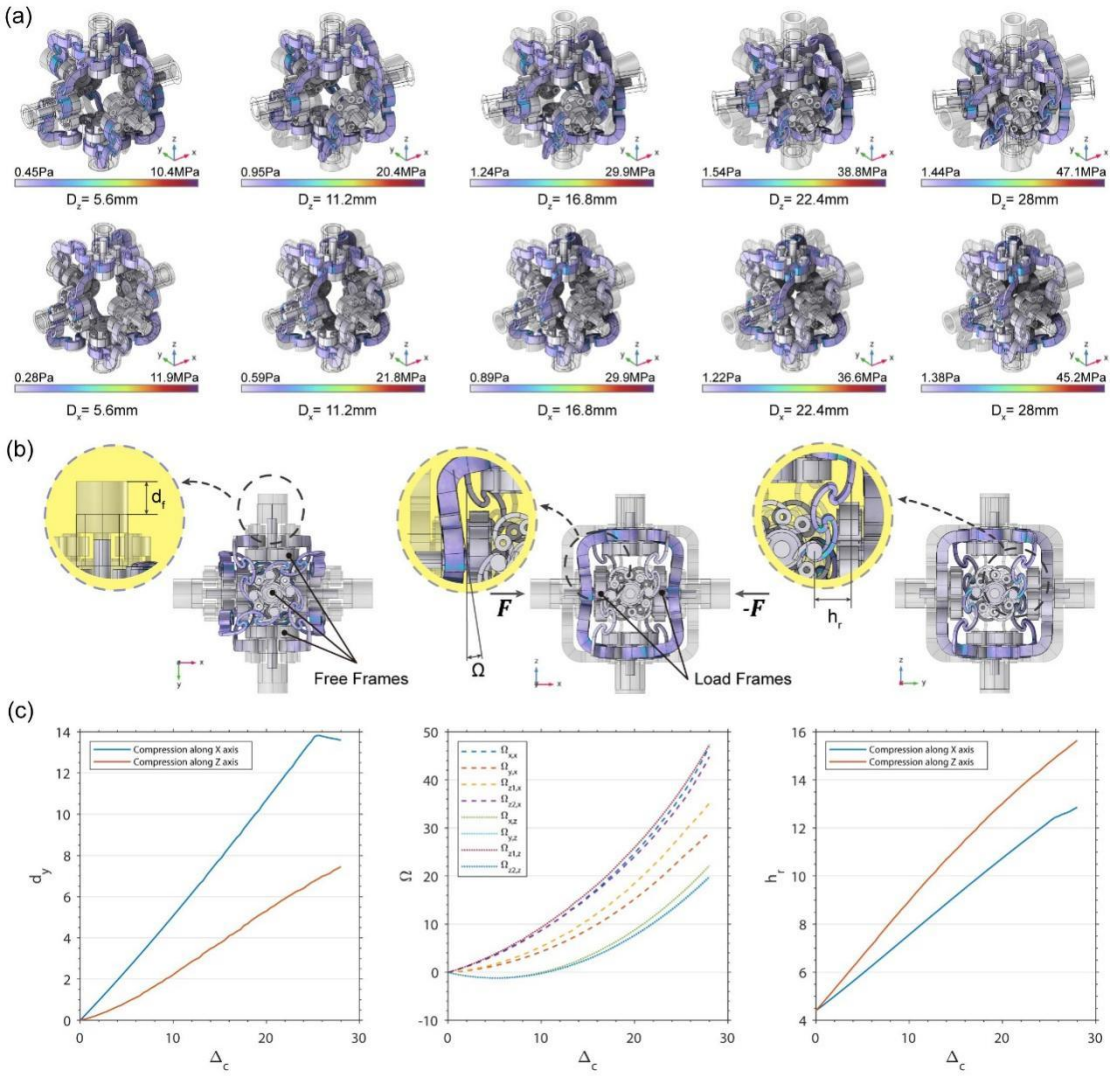

Fig. S5 An investigation of the mechanisms underlying the anisotropic non-linear response of the MCC. (a) Finite element simulation of the MCC at different stages of compression. The load applied to the MCC in the first row is along the Z-axis and in the second row the load is along the X-axis. (b) Graphical depiction of the three characteristic parameters used to describe the deformation of the MCC. (c) From left to right, graphs of the normal displacement of the free frame, the inclination of the load frame connection and the variation of the free frame rotational force arm with compression displacement.

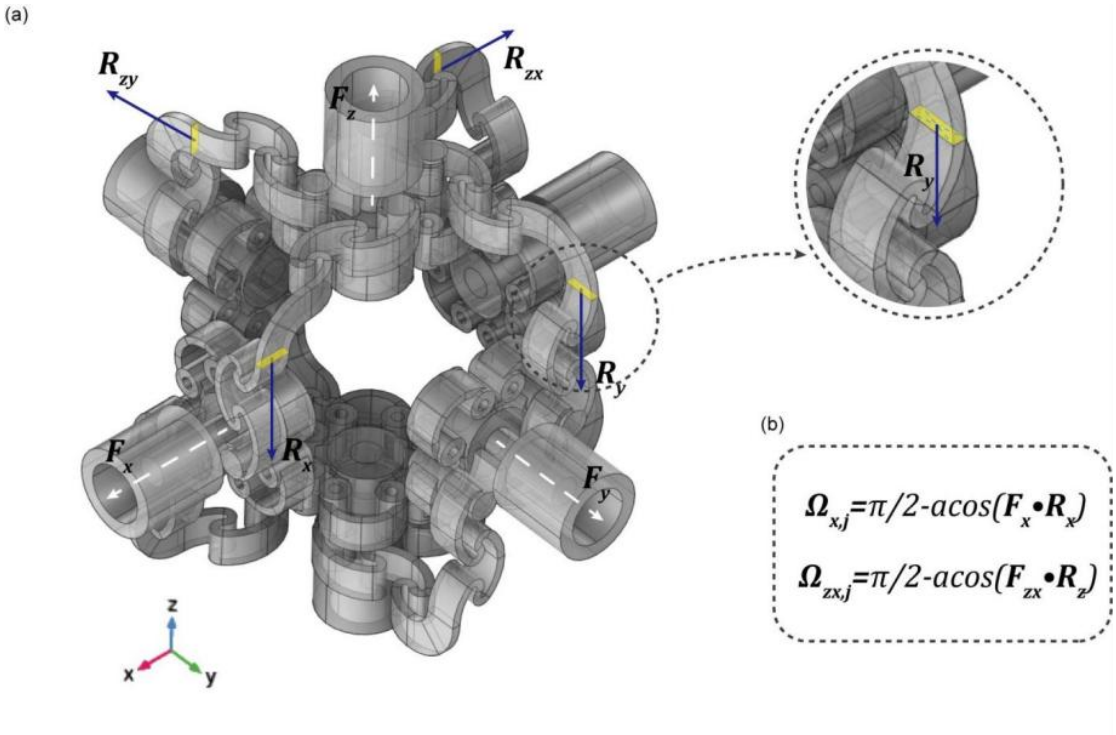

Fig. S6. Detail schematic of the load frame connected to the tilt angle Ω. (a) Definition of the ribbon direction vector R and the load frame normal vector F. (b) Calculated relationship between Ω and R and F.

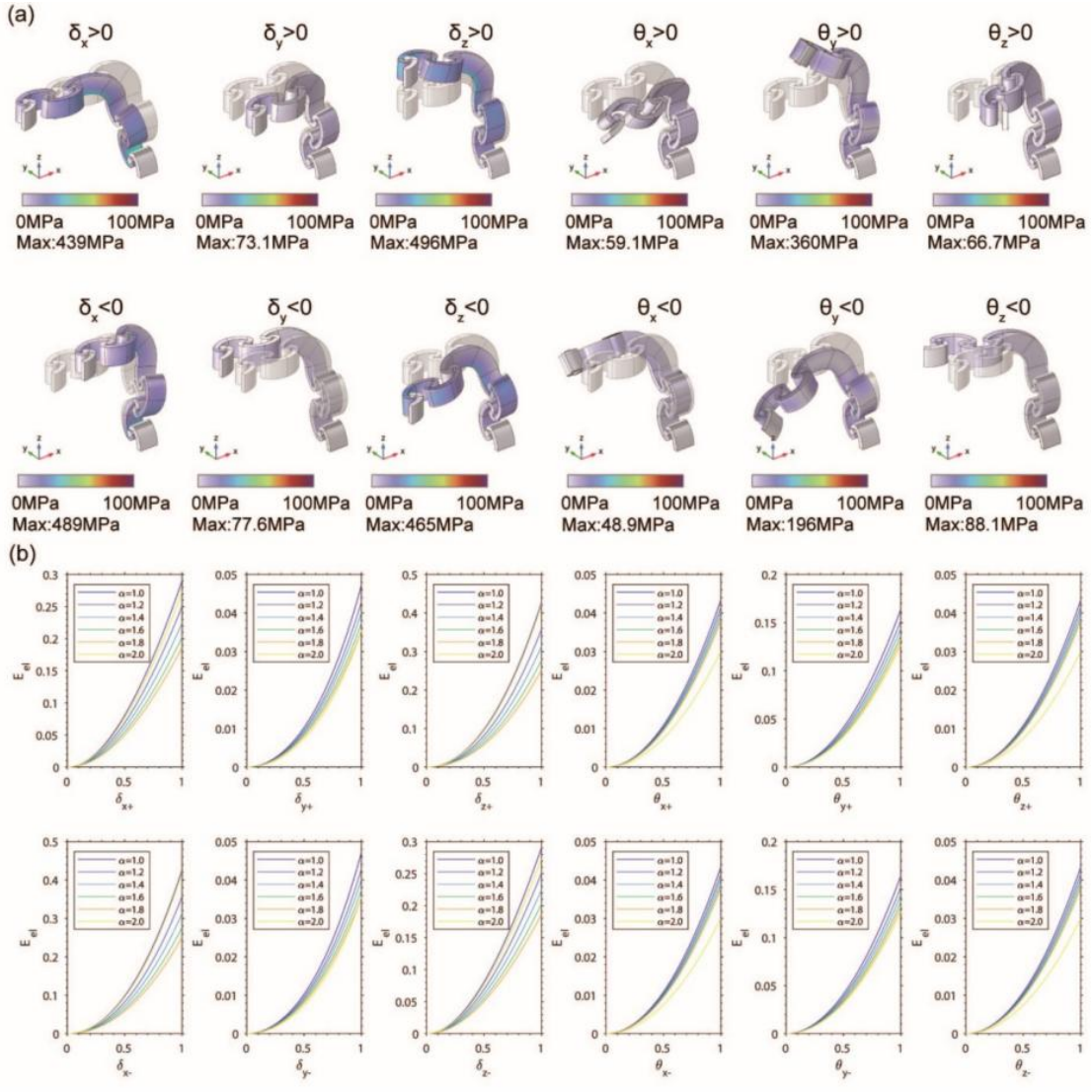

Fig. S7. Numerical simulation results of the ribbon. (a) Deformation diagram and von Mises stress distribution under different boundary displacement conditions. (b) The trend of the elastic energy of the ribbon structure under different values of α corresponding to the above deformation cases.

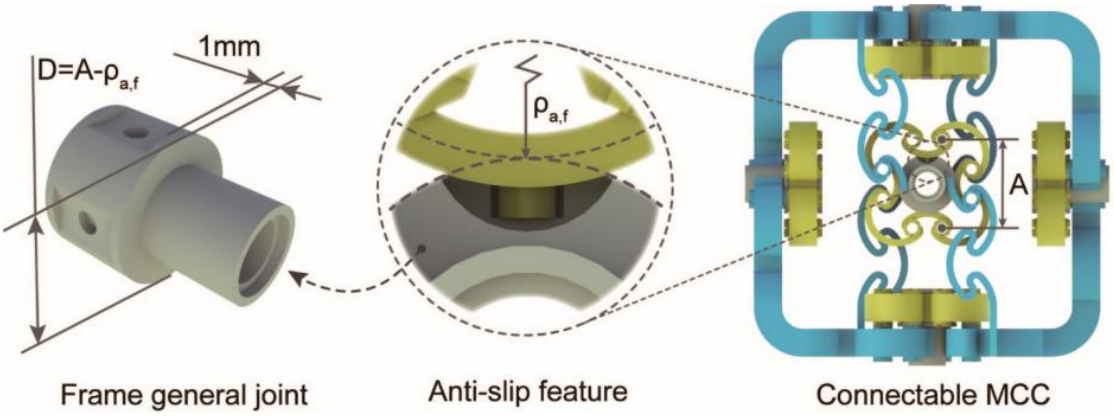

Fig. S8. Design diagram of the generic interface.

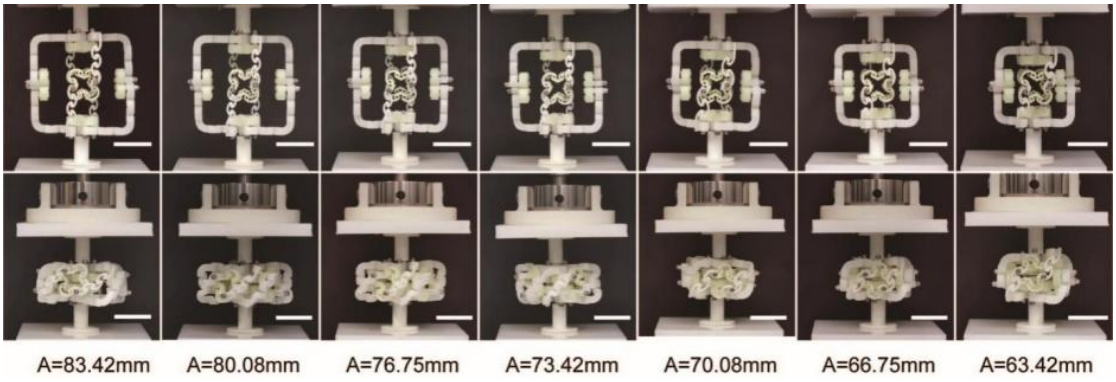

Fig. S9. Deformation performance of the MCC for different A under the condition of fixed a. The length of scale bar in the figure is 40mm.

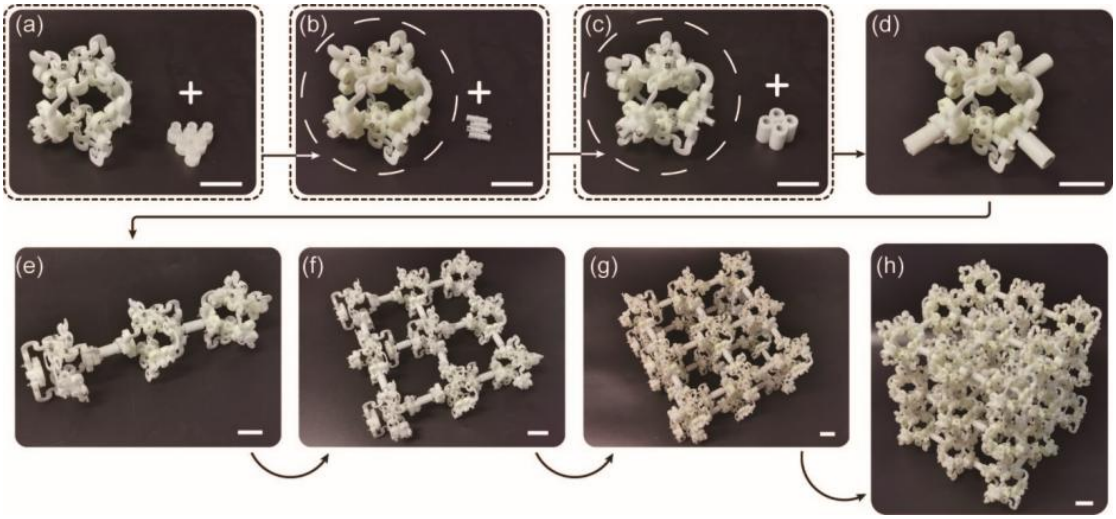

Fig. S10. Procedure diagram of assembling APRMM. The first step (a-b): Six universal interfaces are assembled into one MCC at the center of each frame. The second part (b-c): insert six LEGO parts (1x2 smooth pin 3673) into the six general joints. Step three (c-d): Install the connecting tubes into the above parts. Step 4 (d-e): Assemble the three MCCs into a one-dimensional bar along the X-axis through the 2 connecting tubes. Step 5 (e-f): Similarly, 9 MCCs are connected into a 3×3 two-dimensional sheet by 12 connecting tubes. The sixth step (f-g) repeats the above steps and stacks two 3 × 3 two-dimensional sheets along the Z-axis. The final step (g-h) is assembled on the above basis to form a 3×3×3 3D block AAPRMM. the length of the scale bar in the figure is 20 mm.

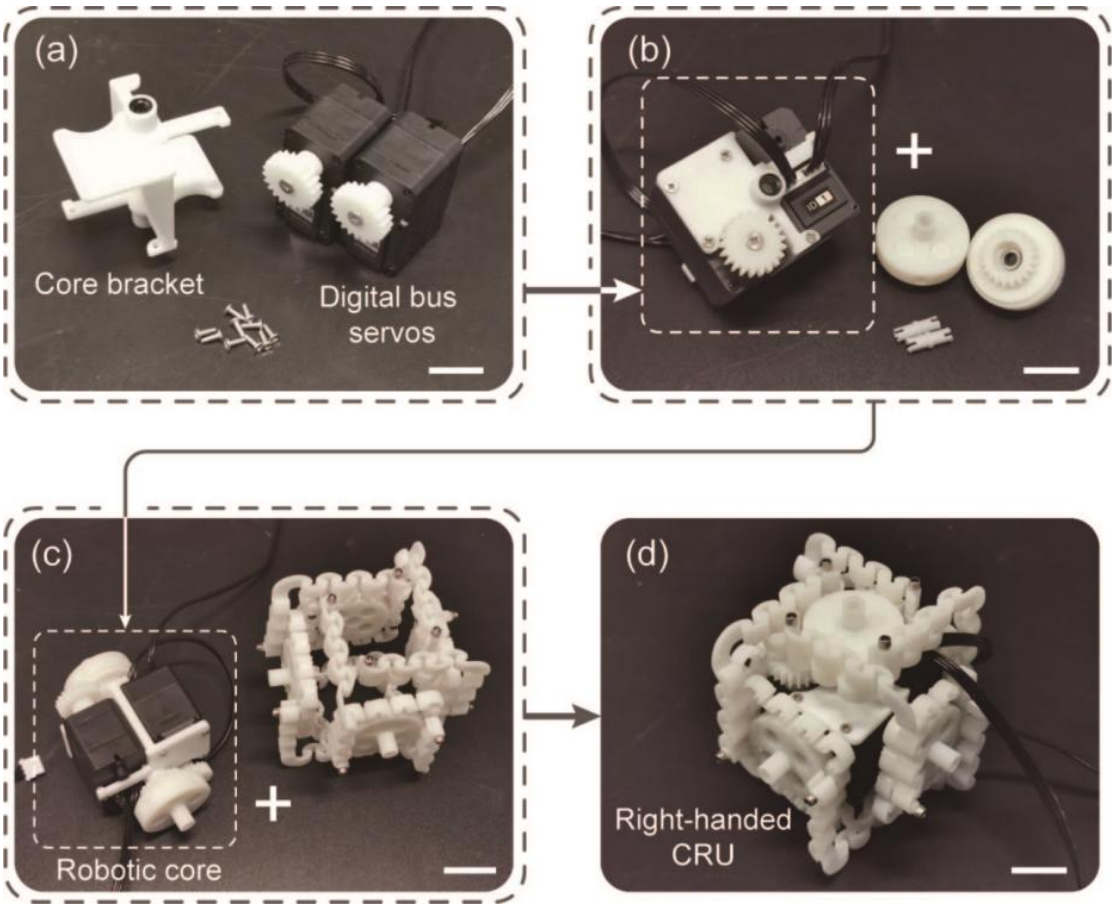

Fig. S11. Procedure diagram for assembling CRU. Step 1 (a-b): Two digital bus servos are connected to the core bracket through standard parts to become the core power component body. The second step (b-c): install the non-standard gear set to the corresponding position of the servos and brackets. The third part (c-d): install the core power component into the shell MCC to form the CRU. the length of scale bar in the figure is 20mm.

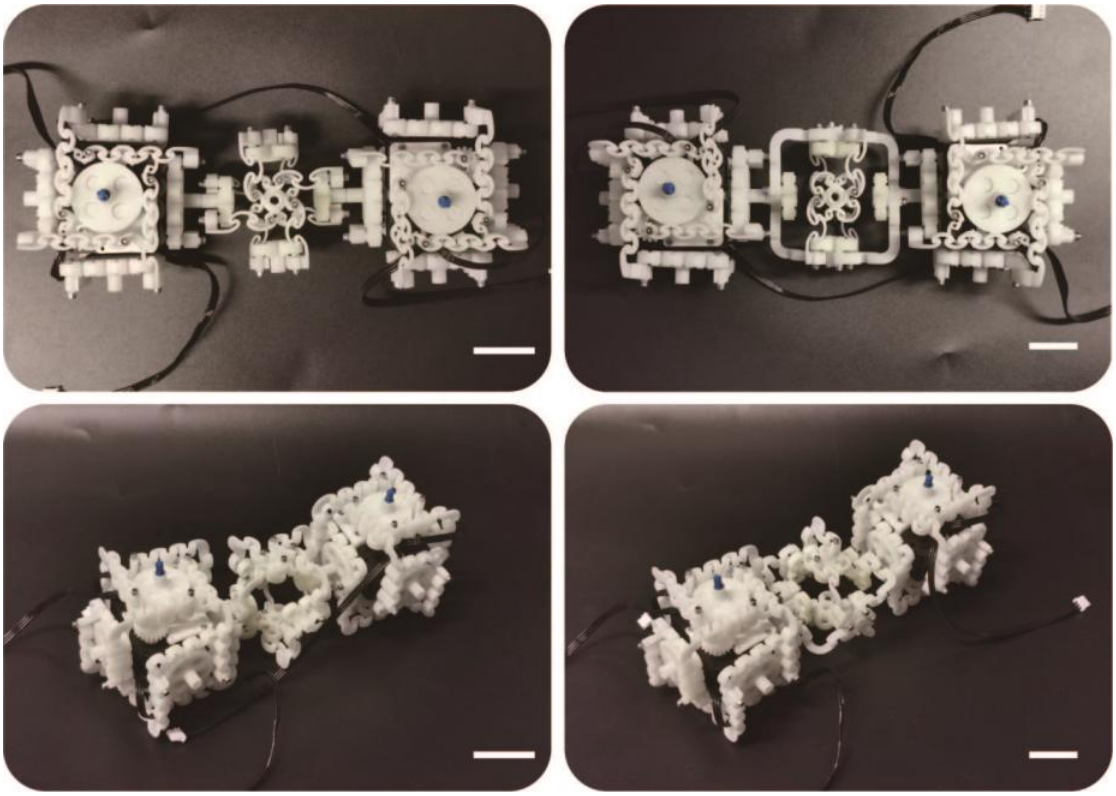

Fig. S12. Physical diagram of the two eCRUPs. The eCRUP-I is shown in the second column on the left and the eCRUP-II in the second column on the right. the length of the scale bar in the figure is 35 mm.

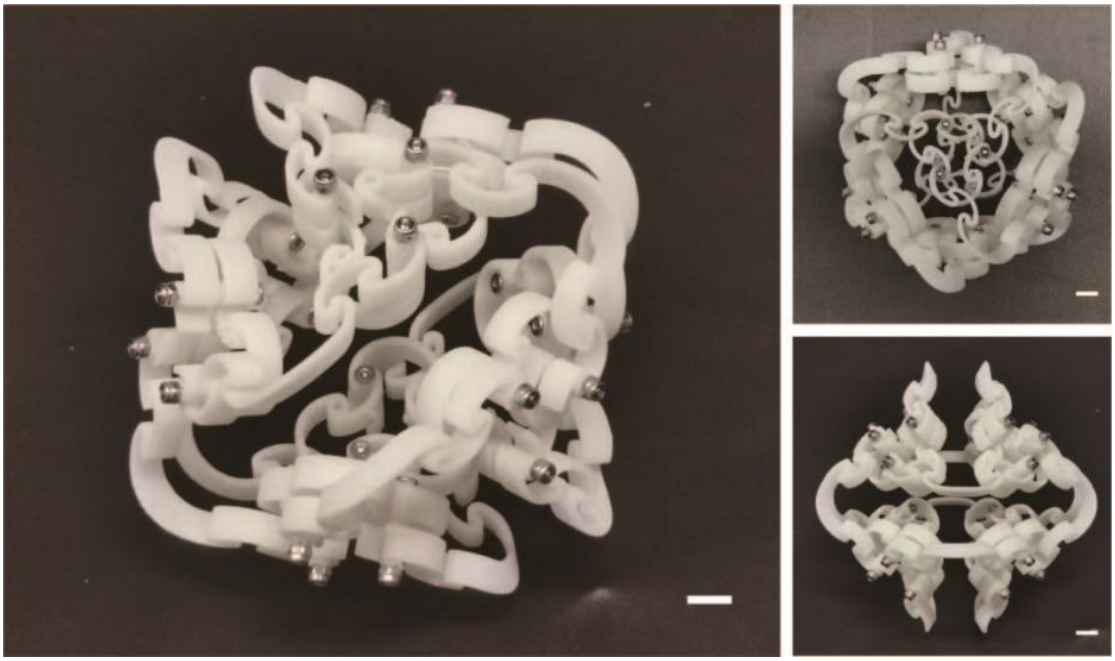

Fig. S13. Physical diagram of the modular compliant octahedron. The length of scale bar is 6 mm.

4 Movies

Movie S1: Uniaxial compression test on different types of MCCs

Movie S2: Uniaxial compression test on resilient metamaterials with different pre-rotation angles**.**

Movie S3: Anisotropic responses of MCC under uniaxial compression.

Movie S4: Anisotropic responses of resilient mechanical metamaterials under uniaxial compression.

Movie S5: Free-falling test of resilient metamaterials.

Movie S6: Trapping test on gradient MCC-based plate.

Movie S7: Energy dissipation test on MCC-based tiled mechanical metamaterials.

Movie S8: Demonstration of CRU deformation.

Movie S9: Linear and turning motion of a CRUP.

Movie S10: Straight-line racing of two eCRUPs.

Movie S11: Demonstration of an eight-legged flexible robot traversing a complex scene.